Journal of Crystal Growth 310 (2008) 5321–5326

Contents lists available at ScienceDirect

Journal of Crystal Growth

journal homepage: www.elsevier.com/locate/jcrysgro

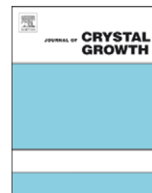

Residual stress relaxation in GaN/sapphire circular pillars measured by Raman scattering spectroscopy

Samuel H. Margueron [a,*], Patrice Bourson [a], Simon Gautier [a], Ali Soltani [b], David Troadec [b], Jean-Claude De Jaeger [b], Andrei A. Sirenko [c], Abdallah Ougazzaden [d]

[a] Laboratoire Matériaux Optiques, Photonique et Systèmes (LMOPS)-CNRS UMR 7132, Université de Metz et SUPELEC, 2 rue Edouard Belin, 57070 METZ, France
[b] Institut d'Electronique, de Microélectronique et de Nanotechnologie (IEMN), Département Hyperfréquence et Semi-conducteurs (DHS), CNRS UMR 8520, Cité Scientifique, Avenue Poincaré, BP 69-59652 Villeneuve d'Ascq, France
[c] Department of Physics, New Jersey Institute of Technology, Newark, NJ 07102, USA
[d] Georgia Institute of Technology/GTL–UMI 2958 Georgia Tech-CNRS, 2-3 rue Marconi, 57070 METZ, France

ARTICLE INFO

Article history:
Received 4 January 2008
Received in revised form
10 September 2008
Accepted 12 September 2008
Communicated by K.W. Benz
Available online 2 October 2008

PACS:
78.30.–j
87.80.Ek

Keywords:
A1. Raman scattering
A1. Residual stresses
A1. Focus ion beam
A1. Stresses
A3. Metalorganic vapour phase epitaxy
B2. Semiconducting gallium compounds

ABSTRACT

Circular pillar structures of various diameters have been prepared by a focused ion beam (FIB) through a 4-μm-thick epitaxial gallium nitride (GaN) film grown on a sapphire substrate. Micro-Raman scattering is used to measure residual stresses based on the shift of an E_2 phonon in the GaN film. Measurements of residual stress profiles are compared to Winkler's elastic formalism for a shear-supported film with proper boundary conditions. The model, optimized at a cleave edge, is compared to the experimental shape of stress variations inside and outside the pillar structures.

© 2008 Elsevier B.V. All rights reserved.

1. Introduction

Residual stresses in wide-gap semiconductor gallium nitride (GaN) layers grown on mismatched substrates, such as sapphire, are known to be detrimental to the performance of microwave power and optoelectronic devices due to the piezo-electric effect in the active region [1]. Current research in this field focuses on the reduction of residual stress by using different substrates for GaN heteroepitaxy [2,3], utilization of nucleation layers [4] or nanoheteroepitaxy [5]. The origins of residual stresses in GaN heteroepitaxial structures are due to lattice and thermal dilation mismatch with the substrate, doping [6–8] or threading dislocation defects formed during the non-equilibrium growth [2,9]. The latter effect is especially important for thick GaN layers, where lattice-mismatch-induced stress relaxes at the vicinity of the substrate.

In this paper, variations of residual stress are made by a focused ion beam (FIB) cuts of pillar structures. The micro-Raman scattering technique is used to measure the shifts of the optical phonon frequency of the E_2 mode for GaN. The main advantage of this approach is the possibility to focus the laser beam to a micron size, while traditional strain measurements (e.g., X-ray diffraction) still remain challenging for microstructures.

2. Sample preparation and measurement technique

A *c*-plane epitaxial 4-μm thick GaN layer was grown on a sapphire substrate using a T-shaped MOVPE reactor [10]. FIB cuts were done with a dual-beam Fei Strata DB 235 apparatus. A gallium gun was used to cut through the 4-μm-thick GaN layer and down to 3 μm inside the sapphire substrate. Pillars with diameters of 1, 2, 5, 10, 20 and 40 μm were prepared using FIB cuts, while the surface was protected by the Pt/Ge metal film. Fig. 1 shows different samples after wet etching. Fig. 2 shows a free-standing structure cut fabricated from an edge of the film by isolating the GaN layer from the sapphire substrate.

* Corresponding author. Tel.: +33 3 87 37 85 64; fax: +33 3 87 37 85 59.
E-mail address: margueron_sam@metz.supelec.fr (S.H. Margueron).

0022-0248/$ - see front matter © 2008 Elsevier B.V. All rights reserved.
doi:10.1016/j.jcrysgro.2008.09.145

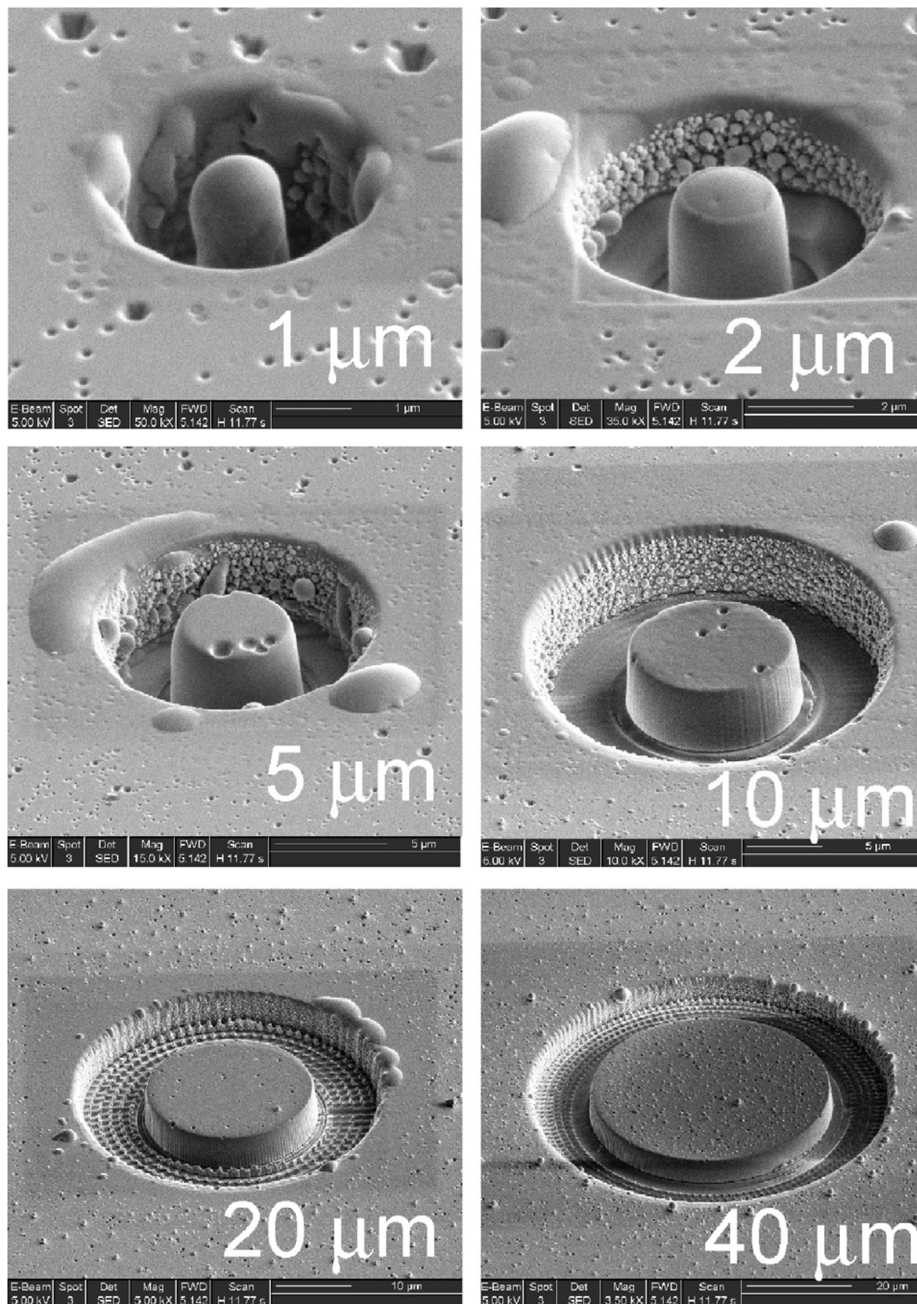

Fig. 1. SEM picture of the GaN/sapphire pillars cuts with 1, 2, 5, 10, 20 and 40 μm diameter.

This pseudo-bulk piece of GaN was kept attached to the GaN film by a tiny bridge for operator convenience.

A backscattering Raman Jobin-Yvon Horiba microprobe spectrometer was used in this study with a 100 × objective (numerical aperture of 0.9), a He–Ne laser with a wavelength of 633 nm, and an X–Y sample stage with an accuracy of 0.3 μm. The excitation power of the laser on the sample was below 0.3 mW/μm^2 to avoid laser-heating effects on the frequency and the full-width half-maximum (FWHM) of the optical phonon lines. Spectra were acquired with a TE-cooled CCD detector using the acquisition time of 300 s per spectrum. Spectra of a neon calibration lamp were measured along with the sample spectra showing no temporal drifts during data acquisition. The frequency accuracy was estimated better than 0.3 cm^{-1}.

The Raman shift of the high-frequency E_2 phonon (at about 568 cm^{-1} [11]) is used in our study. This phonon appears in Raman spectra as an intense band polarized in agreement with the selection rules described in Ref. [11] for the *c*-plane-oriented GaN. As the E_2 phonon is non-polar, it is expected to show no changes with the piezo-electric field. This mode is advantageous in comparison with, for instance, quasi-modes of A_1–E_1 symmetry exhibiting significant Raman shift with the polarization [7].

2.1. Theoretical background

A reduction of stress in GaN layers potentially suitable for devices can be achieved in structures with micrometer-size and free-standing sidewalls produced from continuous GaN films. Modified boundary conditions at the stress-free sidewalls of the pillar structures are expected to result in the stress reduction in the vicinity of the sidewalls as well. However, stress relaxation

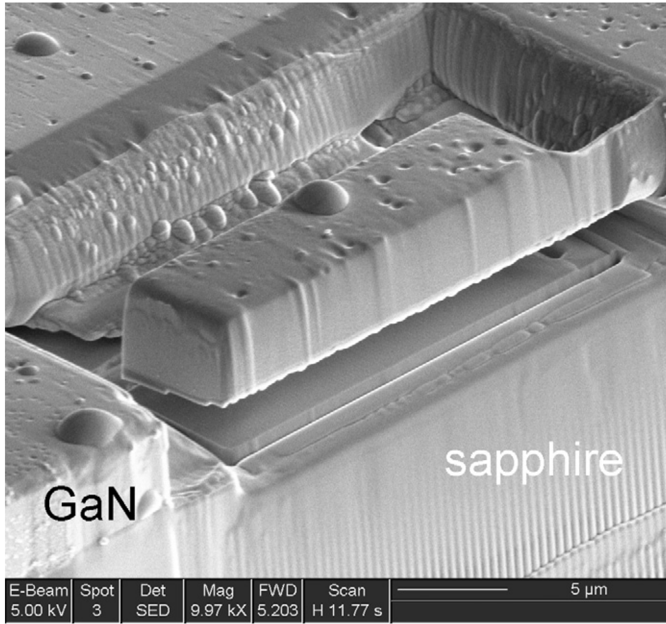

Fig. 2. Pseudo-bulk cuts of a free-standing GaN layer. Cuts have been done on the sides and the bottom to keep the GaN layer intact. GaN remains to be attached to the wafer by a thin bridge.

and pinning due to epitaxial stresses are difficult to model. As a starting point, the approach proposed by Peng et al. [12] can be used to model stress relaxation at the vicinity of circular structures. The model is based on a Winkler elastic formalism, where the GaN film is supported by shear deformation originating from the sapphire substrate. Considering the cylindrical geometry of a membrane-like film (the thickness of the film is much smaller than the diameter of the pillars), the radial strain field $u(r)$ in the film is given by

$$\frac{\partial^2 u(r)}{\partial^2 r}+\frac{1}{r}\frac{\partial u(r)}{\partial r}-\left(\frac{1}{r^2}+\frac{1}{r_0^2}\right)u(r)=0 \tag{1}$$

where the parameter r_0 is determined by the geometry and material properties of the system as follows:

$$\frac{1}{r_0}=\sqrt{\frac{E_{\mathrm{saph}}(1-\nu_{\mathrm{GaN}}^2)}{2(1+\nu_{\mathrm{saph}})E_{\mathrm{GaN}}h_{\mathrm{GaN}}H}} \tag{2}$$

with E_{saph}, ν_{saph} and E_{GaN}, ν_{GaN} are the corresponding Young moduli and Poisson ratios of sapphire and GaN, h_{GaN} the thickness of GaN film, and H the extent of shear deformation in the sapphire substrate. The components of the stress field are given by

$$\sigma_{rr}(r)=\sigma_0+\frac{E_{\mathrm{GaN}}}{(1-\nu_{\mathrm{GaN}}^2)}\left[\frac{\partial u(r)}{\partial r}+\nu_{\mathrm{GaN}}\frac{u(r)}{r}\right] \tag{3}$$

$$\sigma_{\theta\theta}(r)=\sigma_0+\frac{E_{\mathrm{GaN}}}{(1-\nu_{\mathrm{GaN}}^2)}\left[\frac{u(r)}{r}+\nu_{\mathrm{GaN}}\frac{\partial u(r)}{\partial r}\right] \tag{4}$$

$$\sigma_{zz}(r)=0 \tag{5}$$

Peng et al. have solved this expression for circular holes. In Appendix, the solutions for stress field inside and outside of pillars are given with various diameters.

To convert the Raman shift into residual stresses, the standard analysis of deformation potentials in Wurtzite-type structures is used. According to the symmetry-related formalism described by Briggs and Ramdas [13], the shift of the E_2 phonon in function of stresses is given by

$$\Delta\nu_{E2}=a_{E2}(\sigma_{xx}+\sigma_{yy})+b_{E2}\sigma_{zz}\pm c_{E2}\sqrt{(\sigma_{xx}-\sigma_{yy})^2-4(\sigma_{xy})^2} \tag{6}$$

where σ_{ij} is the stress tensor in the Wurtzite basis, and a_{E2}, b_{E2}, and c_{E2} are the stress-related deformation potentials of the E_2 phonon. The literature values of $2a_{E2}$ range from -2.4 [14,15] to $-2.8\,\mathrm{cm^{-1}/GPa}$ [16,17]. The nature of this discrepancy is related to the scattered data of the elastic modulus of GaN. The shear component c_{E2} has been estimated recently to be very weak ($<0.3\,\mathrm{cm^{-1}/GPa}$) [3]. Consequently, this parameter is neglected in the following analysis. Since our study focuses on membrane-type films ($\sigma_{zz}=0$, of Eq. (5)), our consideration is limited to in-plane stresses, we can replace (σ_{xx},σ_{yy}) by (σ_{rr},$\sigma_{\theta\theta}$). The piezospectroscopic shift then reduces to

$$\Delta\nu_{E_2}=a_{E_2}(\sigma_{rr}+\sigma_{\theta\theta}) \tag{7}$$

In the following, Raman shifts are converted into residual stresses using Eq. (7). The value of deformation potential $2a_{E_2}=-2.4\,\mathrm{cm^{-1}/GPa}$ is chosen because of the agreement between experimental and theoretical works [14,15].

3. Experimental results

3.1. Pseudo-bulk of stress-free GaN

In Eqs. (6) and (7), the variation of the Raman shift is determined as the difference between phonon frequencies in stressed and unstressed samples:$\Delta\nu_{E_2}=(x)-\nu_{E_2}^0$ where x is the position of the measurement. The phonon frequency ν_{E2}^0 of an unstressed sample has to be determined on a bulk piece of a similar material. In order to obtain this reference point, we prepared a pseudo-bulk GaN sample from the same wafer. At a cleave edge, a small fraction of the GaN layer was isolated from its substrate using the FIB (Fig. 2). This pseudo-bulk piece revealed a constant Raman position for the E_2 phonon at $567.25\,\mathrm{cm^{-1}}$. In the following, all changes of the Raman shifts will be reported with respect to this value.

3.2. Raman shift at the edge

The Raman shift variation of the E_2 phonon for a line-scan profile at the cleaved edge is plotted in Fig. 3. The right axis of the figure shows the residual stresses, determined according to Eq. (7) with the pseudo-bulk reference. The variation of the stress has been fitted with success by the exponential variation given in Eq. (13) (see Appendix). The fitted coefficients give a relaxation decay of $r_0=9.8\,\mu\mathrm{m}$. The total relaxation occurs for about $3r_0$, which is comparable to the $25\,\mu\mathrm{m}$ relaxation length proposed by Kozawa et al. [18] for the 1–2 µm thick samples.

Using Eq. (2) and the following parameters $E_{\mathrm{GaN}}=E_{\mathrm{saph}}\sim400$ GPa, $\nu_{\mathrm{GaN}}=\nu_{\mathrm{saph}}\sim0.25$ and $h_{\mathrm{GaN}}=4\,\mu\mathrm{m}$, we obtain $H\sim10\,\mu\mathrm{m}$. The depth of shear deformation in the sapphire substrate is about the extent of lateral stress relaxation. This equality is due to the similarity of mechanical properties between GaN and sapphire.

The measurement of the Raman shift between the free-standing GaN and the far field represents a maximal shift of $2.85\,\mathrm{cm^{-1}}$. According to Eq. (7), this value corresponds to a biaxial residual stress of -1.2 GPa.

3.3. Raman shift outside the pillars

Raman shifts measured outside the pillars are shown in Fig. 4 for the 5, 10, 20 and 40 µm diameter cuts. The stress field variation is compared to the solution given by Eqs. (11) and (12). However,

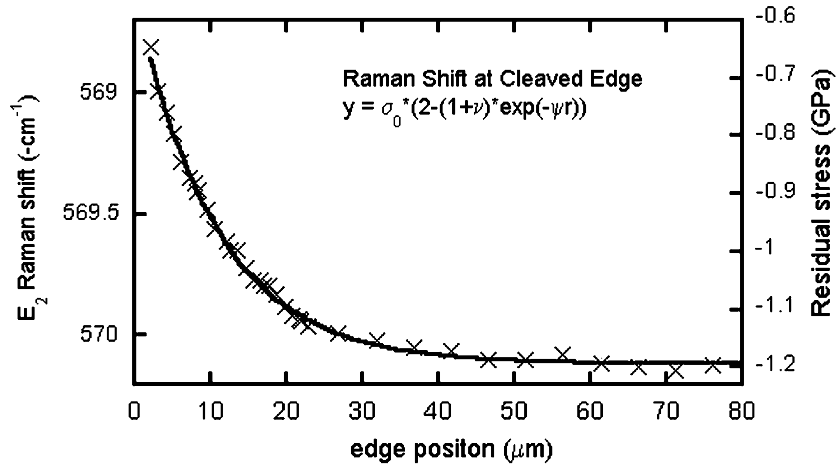

Fig. 3. Raman shift of the E_2 phonon as a function of laser beam position on the top surface. Zero of the horizontal axis corresponds to the edge of the cleaved sample. On the left axis: Raman shift (negative coordinates); on the right axis: residual stresses in GPa given by Eq. (7). The decrease has been fitted by Eq. (13) with $v = 0.27$, $r_0 = 9.8\,\mu\text{m}$ and $r_0 = -1.2\,\text{GPa}$.

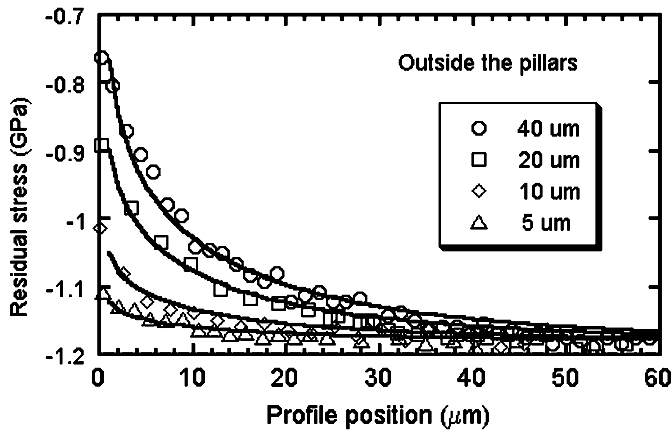

Fig. 4. Raman shift measured outside the pillars from the edge (at the origin) to the far field. Four diameters are represented: 5, 10, 20 and 40 μm. The curves were obtained from Eqs. (11) and (12) with effective diameter $2r_0$ equal to 8, 12, 19 and 26 μm.

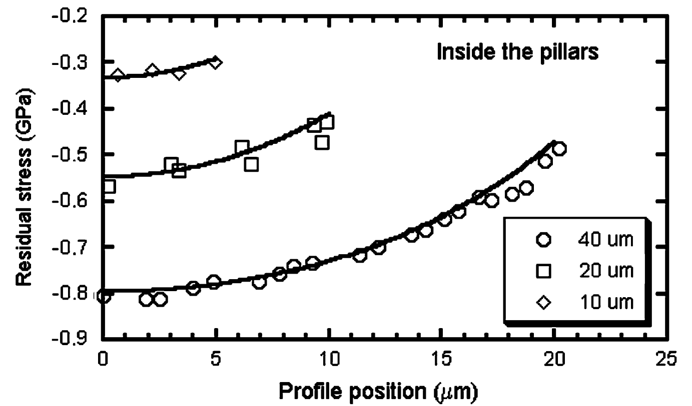

Fig. 5. Profile of Raman shift measured inside the pillars from the center (at origin) to the pillar edge. Three diameters are represented: 10, 20 and 40 μm. The curves were obtained from Eqs. (16) and (17) with a residual stress value in the center of the pillars adjusted as shown in Fig. 6.

an effective radius R has been adjusted to reproduce each set of data. The effective radius was found to be $2r_0$ equal to 8, 12, 18 and 26 μm for the 5, 10, 20 and 40 μm diameter cuts, respectively. One can note that the calculated radius underestimates the real value for the larger pillar diameters. Some reasons of this discrepancy will be discussed in Section 4.

3.4. *Raman shift inside the pillars*

Raman shifts measured inside the pillars are shown in Fig. 5. Only 10, 20 and 40 μm diameter cuts are represented, because for a smaller diameter no profile could be determined. Fig. 5 shows the solutions given by Eqs. (16) and (17) for different radii. The value of residual stresses at the center of the pillar has been adjusted to get the best fit with experimental data. A very good agreement of stress profile is then observed inside the pillars.

4. Discussion

4.1. *Thermal stress contribution*

The amount of residual stress relaxation between far field and pseudo-bulk piece is, to our knowledge, an original and reliable estimation of film/substrate stresses. The pseudo-bulk piece has undergone the same elaboration conditions as any other spot of our GaN/sapphire sample. Also, any implantation or amorphization [6–8] would be limited as compared to the size of the pseudo-bulk piece ($\sim 5 \times 15\,\mu\text{m}^2$). From this experiment we found a $2.85\,\text{cm}^{-1}$ shift in the film, which corresponds to $-1.2\,\text{GPa}$ biaxial stress.

Theses values can be compared to the thermal stress originating from thermal expansion mismatch between the sapphire substrate and the GaN layer. The thermal stress in the GaN layer can be evaluated as follows:

$$\sigma_{\text{GaN,th}} = \frac{E_{\text{GaN}}}{1 - \upsilon_{\text{GaN}}}(\alpha_{\text{GaN}} - \alpha_{\text{Saph}})\Delta T \qquad (8)$$

where ΔT is the difference between the deposition and the ambient temperatures. α_{GaN} and α_{saph} are the thermal dilatation coefficients of GaN and sapphire, E_{GaN} and ν_{GaN} are already defined in Eq. (2). With $\alpha_{\text{GaN}} = 5 \times 10^{-6}\,\text{K}^{-1}$, $\alpha_{\text{saph}} = 8 \times 10^{-6}\,\text{K}^{-1}$ and a deposition temperature of 1000 °C, Eq. (8) gives a compressive residual stress of about $-1.1\,\text{GPa}$ in GaN films on sapphire. This simple evaluation corresponds roughly to the residual stresses measured between the pseudo-bulk and the far field in our experiments.

Meanwhile, the lattice mismatch of the GaN/sapphire is strong (about 13%). The relaxation of the epitaxial layer during

high-temperature growth generates dislocations and a stress gradient through the thickness of the GaN film [1]. A measurement through the cross-section from the top GaN layer to the sapphire interface was carried out. No variation of the Raman shift and phonon line width was observed along the cross-section for all Raman-active modes. We believe that the relaxed thickness is small enough for being detected in Raman scattering experiments with a laser beam size of ~1 μm.

4.2. Residual stress corrections in the pillars

Stress relaxation inside the pillar was not taken into account by the calculated values from Eqs. (16) and (17). In order to include this discrepancy, the values at $r = 0$ were shifted to the measured values. Fig. 6 shows the residual stress measured at the center of the pillar and the values expected from the calculation with the parameters r_0 given at the edge of the sample. A significant difference is found between experimental and calculated values. The experimental data give an exponential variation with pillar diameters with a relaxation distance of about 34 μm. This value appears to be about twice the one determined at the edge, as expected by a relaxation in two directions from the center of the pillars ($2 \times 9.8\,\mu m^2$).

Meanwhile, the model predicts a sigmoid variation with the pillar diameter. The experimental data suggest a faster building stress for small diameters than predicted. This difference may be accounted by the membrane-like approximation. In fact, this later approximation neglects the volume deformation of the pillar and supposes an infinitely deep cut. Indeed, we have determined the penetration depth of shear deformation, H, to ~10 μm, which is larger than the experimental value of the FIB cut through the sapphire substrate (~3 μm).

4.3. Residual stress and Raman width

Another finding is the change of the FWHM of the Raman lines with the residual stress in Fig. 7. Experimental measurements at low laser power density confirm that it was not due to laser-heating phenomena. Fig. 7 represents a linear decrease of FWHM with increasing compressive stresses except at low stresses where we assumed that the anomaly is due to the convolution of stress field variations in the small-diameter pillars with the laser probe size. The decrease of the FWHM is an original finding. For instance, Kozawa et al. [18] found an increase of phonon FWHM

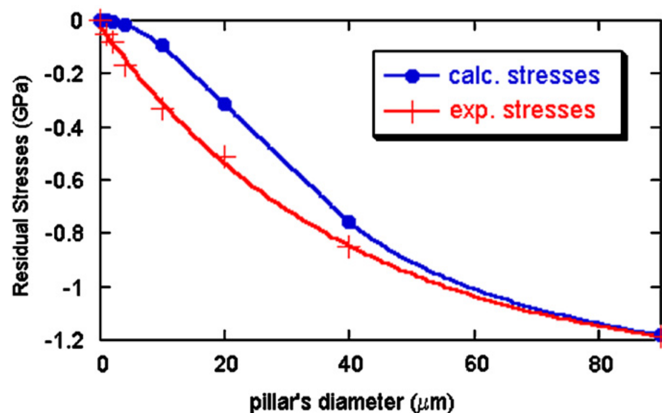

Fig. 6. Experimental and calculated residual stresses in the center of the pillars as a function of diameter except for 150 μm, which corresponds to the far-field measurement far away to any FIB cuts and edges. The building stresses in the film are faster than the one calculated especially for small pillars. Experimental data are fitted by an exponential function with a length decay of 34 μm.

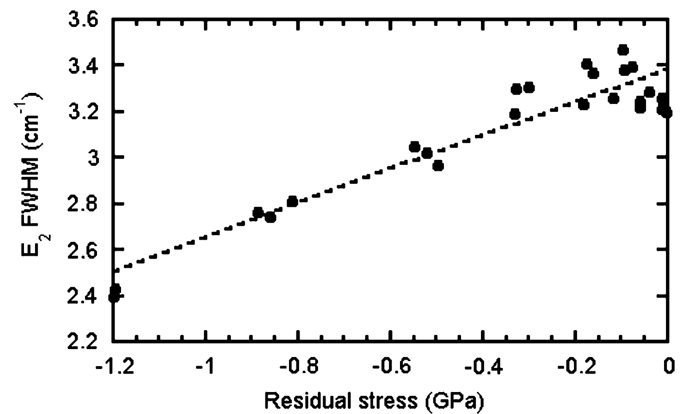

Fig. 7. Experimental width (FWHM) of the E_2 phonon as a function of residual stresses. The increase in Raman width for the small diameter may result from stress convolution with the laser probe. The linear fit (dot line) is a guide for the eyes.

with compressive stresses in the case of GaN layers of different thicknesses, whereas Klose et al. [19] did not observe any change in Raman width with applied stresses.

An explanation for the increase of Raman width can be related to an inhomogeneous strain field release through the film due to dislocation and defects [2,9]. In fact, we point out that a large relaxation has happened due to epitaxial deposition. However, such a relaxation would probably not give a linear relation between residual stress and FWHM. This effect remains challenging to confirm by standard techniques such as transmission electron microscopy (TEM) due to the perturbation of sample preparation and stress relaxation. Another explanation is the increase of phonon lifetime with biaxial stress in the *ab* plane. This point would be original and necessitates to be confirmed.

5. Conclusion

This work focuses on the influence of epitaxial stress in highly constrained structures. An original method of the gradual variation of residual stresses in epitaxial layers is presented. This method utilizes modified boundary conditions for pillar structures prepared by the FIB. Raman shift of E_2 phonons is used for the measurement of residual stresses inside the pillars. A comparison with an elastic model for a shear-supported film shows some discrepancy that may originate from plastic relaxation in the film. Meanwhile we are able to scale perfectly the model to reproduce stress variations in the pillar structures. The use of micro-Raman spectrometry may gain more importance to separate elastic and plastic relaxations.

Acknowledgements

The authors would like to thank the French Foreign Ministry which sponsored part of this work under the program ARCUS. The authors also thank the anonymous reviewer of the paper who has revised several points and improved the discussion of the paper.

6. Appendix

Here we present analysis of the strain and stress fields inside and outside the pillar for a thin film supported by a shear force. The geometry of the calculation is given in Fig. 8. The GaN film is supposed to be thin as compared to both the sapphire substrate

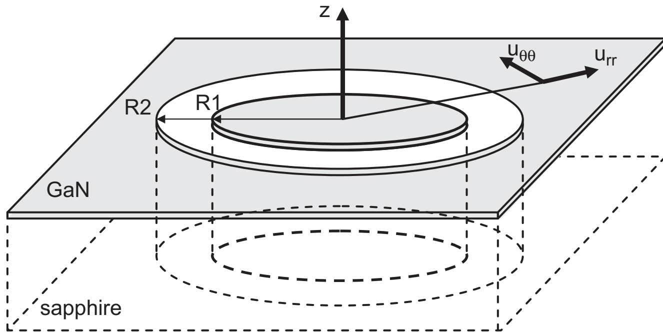

Fig. 8. Cylindrical geometry of the pillar.

and the radius R ($R1$ or $R2$) of the pillars. The cut is supposed to be infinitely deep. The solution of Winkler elastic formalism equations (1)–(5) is given in the following for different boundary conditions.

7. Outside the pillar

The solution of Eqs. (1)–(5) outside the pillar has been developed by Peng et al. [12] where ψ in the original paper was replaced by r_0. Setting the boundary conditions $u(r \to \infty) = 0$ and $\sigma_{rr}(r = R) = 0$, the strain field is given by

$$u(r) = CR\frac{(1 - \nu^2)\sigma_0}{E}K_1(r/r_0) \tag{9}$$

where $K_1(x)$ is the modified Bessel function of the second kind and C is a constant given by

$$C = \frac{1}{[R/r_0K_0(R/r_0) + (1 - \nu)K_1(R/r_0)]} \tag{10}$$

The radial and tangential stress fields are then given by

$$\sigma_{rr}(r = R) = 0 = \sigma_0\left(1 + CR\left[-1/r_0K_0(R/r_0) + (\nu - 1)\frac{K_1(R/r_0)}{R}\right]\right) \tag{11}$$

$$\sigma_{\theta\theta}(r) = \sigma_0\left(1 + CR\left[-\nu/r_0K_0(r/r_0) + (1 - \nu)\frac{K_1(r/r_0)}{r}\right]\right) \tag{12}$$

As pointed out by Peng et al., the solution for $R \to \infty$ shows an exponential behavior

$$\sigma_{\theta\theta}(r) + \sigma_{rr}(r) \approx \sigma_0(2 - (1 + \upsilon)\mathrm{e}^{-r/r_0}) \tag{13}$$

This solution corresponds to a cleaved edge.

8. Inside the pillars

The solution of Eqs. (1)–(5) inside the pillar was calculated with the limit conditions $u(r = 0) = 0$ and $\sigma_{rr}(r = R) = 0$. The strain field is given by

$$u(r) = CR\frac{(1 - \nu^2)\sigma_0}{E_{ox}}I_1(r/r_0) \tag{14}$$

where I_1 is the modified Bessel function of the second kind and C is a constant given by

$$C = \frac{-1}{[R/r_0I_0(R/r_0) + (\nu - 1)I_1(R/r_0)]} \tag{15}$$

The radial and tangential stress fields are then given by

$$\sigma_{rr}(r) = \sigma_0\left(1 + CR\left[1/r_0I_0(r/r_0) + (\nu - 1)\frac{I_1(r/r_0)}{r}\right]\right) \tag{16}$$

$$\sigma_{\theta\theta}(r) = \sigma_0\left(1 + CR\left[\nu/r_0I_0(r/r_0) + (1 - \nu)\frac{I_1(r/r_0)}{r}\right]\right) \tag{17}$$

References

[1] S.C. Jain, M. Willander, J. Narayan, R. van Overstraeten, J. Appl. Phys. Appl. Phy. Rev. 87 (2000) 965.
[2] N. Faleev, H.T.I. Ahmad, M. Holtz, Yu. Melnik, J. Appl. Phys. 98 (2005) 123508.
[3] V. Darakchieva, T. Paskova, M. Schubert, H. Arwin, P.P. Paskov, B. Monemar, D. Hommel, M. Heuken, J. Off, F. Scholz, B.A. Haskell, P.T. Fini, J.S. Speck, S. Nakamura, Phys. Rev. B 75 (2007) 195217.
[4] T.L. Song, S.J. Chua, E.A. Fitzgerald, P. Chen, S. Tripathy, Appl. Phys. Lett. 83 (2003) 1545.
[5] D. Zubia, S.D. Hersee, J. Appl. Phys. 85 (1999) 6492.
[6] D. Alexson, L.B. Mitra Dutta, K.W. Kim, S. Komirenko, R.J. Nemanich, B.C. Lee, M.A. Stroscio, SeGi Yu, Physica B 263–264 (1999) 510.
[7] H. Harima, J. Phys.: Condens. Matter 14 (2002) R967.
[8] M. Katsikini, E.C. Paloura, K. Papagelis, S. Ves, J. Appl. Phys. 94 (2003) 4389.
[9] G. Nootz, A. Schulte, L. Chernyak, A. Osinsky, J. Jasinski, M. Benamara, Z. Liliental-Weber, Appl. Phys. Lett. 80 (2002) 1355.
[10] S. Gautier, C. Sartel, S. Ould-Saad, J. Martin, A. Sirenko, A. Ougazzaden, J. Crystal Growth 298 (2007) 428.
[11] T. Azuhata, T. Sota, K. Suzuki, S. Nakamura, J. Phys. Condens. Matter 7 (1995) L129.
[12] X. Peng, N. Sridhar, D.R. Clarke, Mater. Sci. Eng. A 380 (2004) 208.
[13] R.J. Briggs, A.K. Ramdas, Phys. Rev. B 13 (1976) 5518.
[14] J.W. Ager III, G. Conti, L.T. Romano, C. Kisielowski, MRS Symposium Proceedings 482 (1998) 769.
[15] J.-M. Wagner, F. Bechstedt, Phys. Status Solidi (b) 234 (2002) 965.
[16] P. Perlin, C. Jauberthie-Carillon, J.-P. Itie, A. San Miguel, I. Gorczyca, A. Polian, Phys. Rev. B 45 (1992) 83.
[17] F. Demangeot, J. Frandon, M.A. Renucci, O. Briot, B. Gil, R.L. Aulombard, Solid State Commun. 100 (1996) 207.
[18] T. Kozawa, T. Kachi, H. Kano, H. Nagase, N. Koide, K. Manabe, J. Appl. Phys. 77 (1995) 4389.
[19] M. Klose, G.C. Rohr, N. Wieser, R. Dassow, F. Scholz, J. Off, J. Crystal Growth 189–190 (1998) 634.